A Robust Reception of IEEE 802.15.4a IR-TH UWB in Dense Multipath and Gaussian Noise

Farah Haroon, *Member, IEEE,* Haroon Rasheed, *Member, IEEE,* and Kazi M Ahmed, *Member, IEEE*

Abstract—IEEE 802.15.4a impulse radio-time hopping ultra wide band (IR-TH UWB) physical layer, due to small duty cycle and very short pulse widths is robust against multipath propagation. However, scattering and reflections with the large number of obstacles in indoor channel environments, give rise to dense multipath fading. It imposes serious problem to optimum Rake receiver architectures, for which very large number of fingers are needed. Presence of strong noise also affects the reception of fine pulses having extremely low power spectral density. A robust SRake receiver for IEEE 802.15.4a IR-TH UWB in dense multipath and additive white Gaussian noise (AWGN) is proposed to efficiently recover the weak signals with much reduced complexity. It adaptively increases the signal to noise (SNR) by decreasing noise through a recursive least square (RLS) algorithm. For simulation, dense multipath environment of IEEE 802.15.4a industrial non line of sight (NLOS) is employed. The power delay profile (PDF) and the cumulative distribution function (CDF) for the respective channel environment are found. Moreover, the error performance of the proposed architecture is evaluated in comparison with conventional SRake and AWGN correlation receivers. The simulation results indicate a substantial performance improvement with very less number of Rake fingers.

Keywords—Adaptive noise cancellation, dense multipath propagation, IEEE 802.15.4a, IR-TH UWB, industrial NLOS environment, SRake receiver

I. INTRODUCTION

A carrier less, baseband physical layer (PHY) of impulse radio-time hopping ultra wide band (IR-TH UWB) is approved as [1]. The allowable frequency range is classified into a sub GHz, low (3.1 to 4.8 GHz) and high (6.0 to 10.6 GHz) band plans. Both GHz bands are further divided into 15 operating channels, each identified by a distinct center frequency and bandwidth. The $M = 4$ symbols of IEEE 802.15.4a IR-TH UWB rely on M burst position modulation-binary phase shift keying (BPM-BPSK) modulated biorthogonal signals. Independent time hopping (TH) codes of different data streams allow multiple access communication without catastrophic collisions. The small duty cycle and very short pulse widths reduce intersymbol interference (ISI) and the inherent discontinuity mitigates the effects of constant interventions. It has strong potential against multipath fading, but due to fine time resolution and increased bandwidth, the scatterers and reflectors in non line of sight (NLOS) indoor surroundings generate a plenty of resolvable multipath components (MPCs). The situation is typically severe in industrial NLOS environment, where the presence of large metallic enclosures causes severe small scale fading and a dense power delay profile (PDP). To exploit this multipath diversity, a very large number of Rake fingers are needed for coherent reception.

Uptill now, the performance evaluation of IEEE 802.15.4a IR-TH UWB in dense multipath channels was mostly targeted towards positioning and acquisition as in [2] and [3]. Reception and error performance was also focused either over AWGN [4] or sparse residential and office environments [5]-[7]. However, simulations in [8] were carried out in dense IEEE 802.15.4a industrial NLOS environment available as channel model 8 (CM8). In the presence of large excess delays, the first ray does not carry the largest amplitude and hence selective-Rake (SRake) utilizing the strongest MPCs was employed instead of all-Rake (ARake) and partial-Rake (PRake) receivers. The results indicated an obligation of hundreds of fingers, but no solution to solve this problem is yet proposed.

In this paper, the error performance of SRake reception in dense multipath propagated IEEE 802.15.4a industrial NLOS environment of CM8 is focused. The channel impulse response and the respective PDP is generated. Using different number of strongest MPCs, the signal to noise ratio (SNR) statistic of the channel is evaluated and the respective CDFs are obtained. The adaptive noise cancellation principle of [9] commonly applied on voice signals is introduced with conventional SRake reception of IR-TH UWB signals. The proposed adaptive SRake architecture overcomes the complexity indicated in [8]. It cancels the noise from weak UWB signals and improves the SNR through an adaptive recursive least square (RLS) algorithm. The error performance is evaluated, which shows a significant improvement as compared to conventional SRake and AWGN correlation receivers.

The rest of the paper is organized as follows. Multipath propagation in IR-UWB is discussed in Section II. Section III gives an overview of the system model with complete description of signal construction and dense industrial NLOS channel. Robust receiver architecture is specifically proposed in Section IV. Results along with simulation detail are presented in Section V. Section VI concludes the final remarks.

II. MULTIPATH PROPAGATION IN IR-UWB

Multipath propagation causes an accretion of several delayed, attenuated and distorted replicas of the transmitted signal at the receiver. Each kth MPC generated due to interaction with the surroundings is inherited with an amplitude a_k, phase ϑ_k and delay τ_k. If the delay difference of two MPCs satisfies Eq.(1), they are said to be resolvable.

$$| \tau_b - \tau_c | \gg \frac{1}{B} \quad (b \neq c) \tag{1}$$

Farah Haroon, Haroon Rasheed and Kazi M. Ahmed are with the Telecommunications Field of Study, Asian Institute of Technology, Klong Luang, Pathumthani 12120, Thailand, email: (Farah.Haroon,Haroon.Rasheed,kahmed)@ait.ac.th
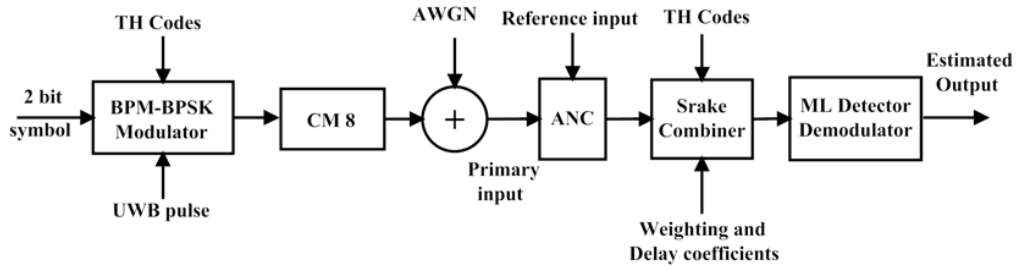
Fig. 1. System Model indicating the reception of BPM-BPSK modulated IR-TH UWB signal through robust SRake receiver

All such K resolvable MPCs collectively define the channel impulse response as

$$h(t) = \sum_{k=0}^{K-1} a_k \, e^{j\vartheta_k} \delta(t - \tau_k) \tag{2}$$

However, the above equation best suits for carrier modulated signals, in which complex baseband technique is used to express the channel impulse response and the reception involves the generation of in phase and quadrature signals [10]. Comparatively in carrier less baseband IR-UWB, using pulse based transmitter and receiver, the channel impulse response is represented as a real pass band system and the phase ϑ is not considered. Due to increased frequency, all the multipath propagation effects in UWB channels become frequency dependent which give rise to distortion ξ_k in each kth path of the received signal. The channel response of Eq.(2) for narrow band systems is no more a Dirac delta function [11], and is represented as

$$h(t) = \sum_{k=0}^{K-1} a_k \, \xi_k(t) * \delta(t - \tau_k) \tag{3}$$

where * denotes convolution.

Under the slow fading assumption of the frequency selective channel, the gain a_k and the delay τ_k are taken constant over a symbol duration. In the presence of AWGN, which is assumed as independent of fading amplitudes a_k with N_0 (W/Hz) as single sided power spectral density, the instantaneous SNR per symbol of kth path having E_s as symbol energy is given by

$$\gamma_k = (a_k^2 E_s)/N_0 \tag{4}$$

and the respective total received instantaneous SNR γ would be $\gamma = \sum_{k=0}^{K-1} \gamma_k$

III. SYSTEM MODEL

Uncoded IEEE 802.15.4a IR-TH UWB is modulated as a two bit symbol using BPM-BPSK employing TH codes. It generates a set of $M = 4$ biorthogonal signals transmitted through dense multipath propagated IEEE 802.15.4a industrial NLOS CM8. The received signal contaminated by strong AWGN and interferences is recovered via proposed robust SRake receiver as shown in Fig. 1. It includes a dual input adaptive noise canceler (ANC), SRake combiner and a maximum likelihood (ML) detector followed by a demodulator.

A. Signal Construction

According to [1], data for coherent detection is modulated as a two bit symbol using BPM-BPSK. It produces a burst of duration T_{burst} using N_{cpb} consecutive pulses with each pulse occupying a small chip interval of T_c = 2 ns. The burst can be present in any of the possible N_{hop} positions identified by independent TH codes. The code represents a sequence $[c_0^q, c_1^q, ..., c_{N_{hop-1}}^q]$ of integers defining respective burst locations in a data stream.

The first data bit d_{jBPM}^{qc} encodes the position of the burst in either half of the symbol duration T_{BPM}, while the second data bit d_{jBPSK}^{qc} indicates its polarity. If E_s is the symbol energy and $p_{tx}(t)$ is the transmitted first derivative Gaussian pulse, $s_{txm}^{qc}(t)$ represents the mth biorthogonal transmitted signal of qth node using c^{th} TH code as

$$s_{txm}^{qc}(t) = \sqrt{\frac{E_s}{N_{cpb}}} \sum_{j=-\infty}^{\infty} (1 - 2d_{jBPSK}^{qc}). \tag{5}$$
$$\sum_{x=1}^{N_{cpb}} p_{tx}(t - c_j^q T_{burst} - xT_c - d_{jBPM}^{qc} T_{BPM})$$

B. Dense Multipath Propagated Industrial NLOS Channel

On behalf of extensive measurement campaigns and simulations, IEEE 802.15.4a offers several channel environments available as channel models (CM1 to CM9). By incorporating path loss, large and small scale fading, they provide realistic channel conditions for design and analysis for both 3 to 10 and below 1 GHz frequency ranges.

The most dense multipath propagated environment is available as industrial NLOS channel model 8. The analysis is based on modified Saleh and Valenzuela (SV) model for indoor multipath propagation, which indicates that the grouping of objects in the surroundings leads to clustering of MPCs. Using a_{kl} and τ_{kl} as the gain and delay of kth component of the lth cluster and T_l as the arrival time of lth cluster, the channel impulse response appears as

$$h(t) = \sum_{l=0}^{L-1} \sum_{k=0}^{K-1} a_{kl} \, \delta(t - T_l - \tau_{kl}) \tag{6}$$

Over a small area complex Gaussian best accounts for their amplitude variations, with an equivalent complex baseband

Rayleigh distribution. However, in the presence of large excess delays prevailing in NLOS industrial, the conventional distribution is no more valid for large number of non resolvable MPCs in each delay bin [12]. Alternatively, Nakagami distribution with probability density function (PDF) shown in Eq.(7) has been suggested for small scale fading with a Lognormally distributed Nakagami m_l factor. The respective distribution is written as

$$pdf(z) = \frac{2}{\Gamma(m_l)} \left(\frac{m_l}{\Omega}\right)^{m_l} z^{2m_l-1} \, exp \left(-\frac{m_l}{\Omega}z^2\right) \quad (7)$$

Where $\Gamma(m_l)$ is the gamma function and Ω is the mean square value of the amplitude.

In other environments, the PDP appears with Poisson distributed cluster and ray arrival times. In contrast, with a single cluster in industrial NLOS channel, PDP is expressed as

$$E\{| \, a_{kl} \, |^2\} \quad = \quad (1 - \chi \, . \, exp \left(-\frac{\tau_{kl}}{\gamma_{rise}}\right)) \quad (8)$$
$$exp \left(-\frac{\tau_{kl}}{\gamma_1}\right) . \frac{\gamma_1 + \gamma_{rise}}{\gamma_1} \frac{\Omega_1}{\gamma_1 + \gamma_{rise}(1-\chi)}$$

Where χ represents the attenuation of first path and γ_{rise} and γ_1 respectively pertaining the rising and decaying time constants.

Apart from the statistics and complete detail of small scale fading available in [13], the phenomenon of diffraction and reflection like in all other channel environments are frequency dependent for which modified path loss functions are considered.

C. Receiver Architecture

We introduce an adaptive noise canceler (ANC) at the front end of SRake combiner. The received signal through CM8 in the presence of AWGN appears at the primary input, while the correlated samples of the primary noise are applied at the other reference input. The ANC adaptively reduces the noise content and feeds the signal to four independent Rake units of the SRake combiner. Each mth Rake unit relates to one of biorthogonal transmitted signals. In addition to weighting and delay coefficients, the matching template also rely on the impulse response of CM8. The Rake output is the decision metric on behalf of which the detector and demodulator provide the estimated symbol.

IV. AN ADAPTIVE SRAKE RECEIVER

All the sections of the proposed receiver architecture with their respective inputs and outputs are mentioned in Fig. 2 as follows

A. RLS Adaptive Noise Canceler

For m^{th} transmitted signal, the respective mutually and statistically independent and identically distributed (iid) additive white Gaussian noise (AWGN) random variable has zero mean and variance given by

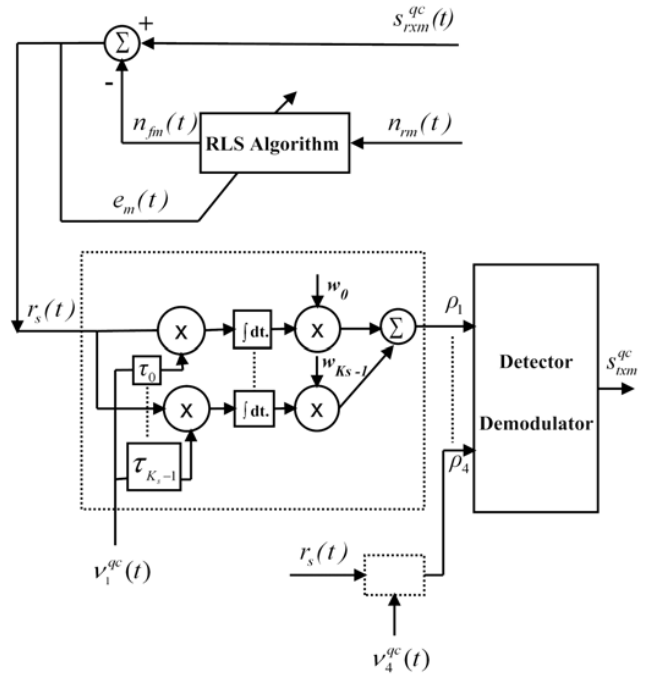$$\sigma_m^2 = \frac{N_o}{2}, \quad m = 1, ..., M \quad (9)$$

Fig. 2. Robust Srake receiver operating in IEEE 802.15.4a industrial NLOS CM8 for $m = 1...M$ biorthogonal signals

While neglecting the antenna effects and assuming $h(t)$ as the impulse response of CM8, the corresponding received signal at the primary input of ANC is represented as $s_{rxm}^{qc}(t)$. If $*$ indicates the convolution operation and $n_{pm}(t)$ as the primary noise added into the mth transmitted signal, $s_{rxm}^{qc}(t)$ is given by

$$s_{rxm}^{qc}(t) = s_{txm}^{qc}(t) * h(t) + n_{pm}(t) \quad (10)$$

Using i as time index, the above equation is written as

$$s_{rxm}^{qc}(i) = s_{txm}^{qc}(i) * h(i) + n_{pm}(i) \quad (11)$$

where $s_{txm}^{qc}(i) * h(i)$ designates our desired response $d_m(i)$. The noise $n_{rm}(i)$, a correlated version of primary noise appears at the reference input as the first tap input $u_m(i)$. After being adaptively filtered through M_w order tap weight vector as $n_{fm}(i)$, it is subtracted from the primary input to produce an error signal $e_m(i)$ at the output of an ANC.

$$e_m(i) = s_{rxm}^{qc}(i) - n_{fm}(i) \quad (12)$$

The noise canceler actually adapts its impulse response through a tap weight vector. It minimizes the squared error via RLS algorithm mentioned in [14]. The filtered noise $n_{fm}(i)$ is adjusted such that the noise power present in the primary input is reduced keeping the signal power unchanged.

Thus, for the length of the observed data y, equivalent to symbol duration, our objective function $\varepsilon_m(y)$ is given by

$$\varepsilon_m(y) = \sum_{i=1}^{y} \beta_m(y, i) \mid e_m(i) \mid^2 \quad (13)$$

To minimize the objective function, the algorithm on the basis of initial known conditions and feed back samples recursively

updates the old estimates of tap weight vector $\mathbf{w_m}(y)$.
During the observation interval $1 \leq i \leq y$ equivalent to symbol duration, the forgetting factor $0 \leq \beta_m(y,i) \leq 1$ of Eq.(14) is introduced to exponentially ignore the effect of past data.

$$\beta_m(y,i) = \alpha_m^{y-i} \tag{14}$$

where α_m is a positive constant close to, or equal to 1. The tap weight vector modifies the error signal according to

$$\mathbf{e_m}(i) = \mathbf{s_{rxm}^{qc}}(i) - \mathbf{w_m}^H(y)\mathbf{n_{rm}}(i) \tag{15}$$

where $\mathbf{s_{rxm}^{qc}(i)}$ indicates the time indexed sampled values of the received signal and $\mathbf{w_m}^H(y)$ at $(t = y)$ represents the conjugate transpose of $\mathbf{w_m}(y)$.
Both the tap weight vector $\mathbf{w_m}(y)$ and the time indexed reference noise vector $n_{rm}(i)$ are expressed as

$$\mathbf{w_m}(y) = [w_{m0}(y), w_{m1}(y), ..., w_{m(M_w-1)}(y)]^T \tag{16}$$

$$\mathbf{n_{rm}}(i) = [n_{rm}(i), n_{rm}(i-1), ..., n_{rm}(i-M_w+1)]^T \tag{17}$$

The optimum value of the tap weight vector, at which our objective function acquires the minimum, is represented as $\hat{\mathbf{w}}_\mathbf{m}(y)$. According to [14], it is the product of the inverse of $\mathbf{\Phi_m}(y)$ and $\theta_\mathbf{m}(y)$ written as

$$\hat{\mathbf{w}}_\mathbf{m}(y) = \mathbf{\Phi_m^{-1}}(y)\theta_\mathbf{m}(y) \tag{18}$$

where $\mathbf{\Phi_m^{-1}}(y)$ is the M_w by M_w time averaged correlation matrix of tap inputs given by

$$\mathbf{\Phi_m^{-1}}(y) = \sum_{i=1}^{y} \alpha_m^{y-i}\mathbf{u_m}(i)\mathbf{u_m}^H(i) \tag{19}$$

and $\theta_\mathbf{m}(y)$ of mth signal is the M_w by 1 time averaged cross correlation vector between the tap inputs and the complex conjugation of desired response $d_m(i)$ indicated as

$$\theta_\mathbf{m}(y) = \sum_{i=1}^{y} \alpha_m^{y-i}\mathbf{u_m}(i)\mathbf{d_m}^*(i) \tag{20}$$

The received signal after being adaptively filtered at the output of ANC is represented as $r_s(i)$. It is applied to the four Rake units, where the resultant increased SNR is effectively utilized to reduce the required number of fingers.

B. SRake Combiner

The branch statistic of SRake combiner was found by generating an impulse response of CM8 using Matlab function uwb-sv-model-ct-15-4a.m provided in [15]. The function provides 100 realizations of channel impulse response $h(t)$ at each sampling interval T_s. Average of $h(t)$ at each sampling interval gives the channel vector $\mathbf{h}$ with the corresponding time index vector $\mathbf{t}$ available in Eq.(21) and Eq.(22) as

$$\mathbf{h} = [h_0(0), h_1(T_s), ..., h_{K-1}(K-1)T_s]^T \tag{21}$$

$$\mathbf{t} = [0, T_s, ..., (K-1)T_s]^T \tag{22}$$

Representing the strength of all the received K MPCs, $\mathbf{h}$ was then sorted for K_s strongest MPCs in $\mathbf{h_s}$ with time index $\tau_\mathbf{s}$ as

$$\mathbf{h_s} = [h_0(\tau_0), h_1(\tau_1), ..., h_{(K_s-1)}(\tau_{K_s-1})]^T \tag{23}$$

$$\tau_\mathbf{s} = [\tau_0, \tau_1, ..., \tau_{(K_s-1)}]^T \tag{24}$$

The above two vectors respectively represent the branch weighting coefficients $\mathbf{w_s}$ and delay elements of SRake combiner.
Each mth Rake unit, uses a set of K_s fingers (branches) enclosed within dashed boxes of Fig. 2.
The locally generated matching template $\nu_m^{qc}(t)$ after neglecting the antenna effects is selected for one complete symbol duration. For m^{th} signal using c^{th} TH code assigned to q^{th} node, it is therefore chosen as

$$\nu_m^{qc}(t) = s_{txm}^{qc}(t) * h(t) \tag{25}$$

Each branch correlates the received signal with the matching template delayed by τ_s and weighted by w_s. The sum of all the branch outputs corresponding to a maximal ratio combiner (MRC) is treated as a decision metric ρ_m as follows

$$\rho_m = \sum_{s=0}^{K_s-1} w_s.C_m(r_s(t), \nu_m^{qc}(t-\tau_s)) \tag{26}$$

where $C_m(a, b)$ represents the correlation between a and b entities.
These ρ_m values for the four biorthogonal signals fed into a detector and a demodulator for final estimation of the transmitted symbol.

C. Detector

Assuming perfectly synchronized transmitter and receiver, the signal detection was analyzed and simulated as a single data stream using c^{th} TH code. The estimated signal $\tilde{s}_{txm}^{qc}(t)$ is based on maximum likelihood (ML) detection where the value of the largest weighted correlation sum decides one of M signals as

$$\tilde{s}_{txm}^{qc}(t) = \arg\max_m | \rho_m | \tag{27}$$

Finally the demodulator provides the corresponding symbol.

V. SIMULATION AND RESULTS

Simulations were carried out in IEEE 802.15.4a industrial NLOS environment of CM8 at a center frequency $f_c = 7.987$ GHz of channel 11 of high band plan. The large center frequency was selected to enhance immunity against dense multipath propagation. With a sampling frequency of $f_s = 50$ GHz, the channel impulse response was generated based on [15]. The average PDP of Fig. 3 produced on behalf of it, clearly shows the dense accumulation of MPCs, with the first arriving component not indicating the largest amount of energy.
Channel realizations of CM8 were generated 1000 times and histograms using 20 and 100 strongest MPCs were obtained. It gives the discrete approximation of the PDFs of the instantaneous received SNR of selected MPCs from which respective
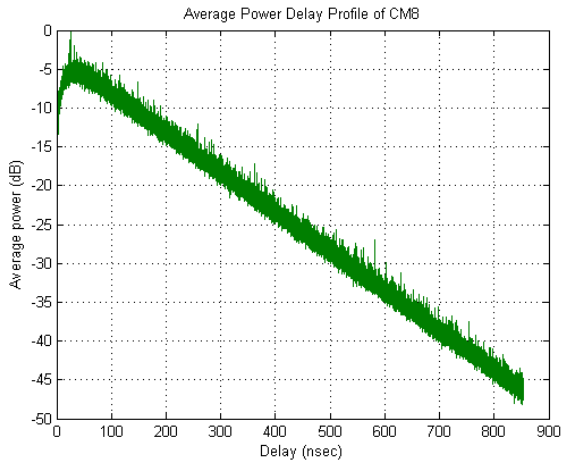
Fig. 3. Power Delay Profile of CM8

Fig. 5. Correlation strength between $n_{pm}(i)$ and $n_{rm}(i)$ vs corrrelation strength between $d_m(i)$ and $r_s(i)$

CDFs were obtained. Fig. 4 indicates that in IEEE 802.15.4a industrial NLOS CM8 following Nakagami distribution for small scale fading, an approximate gain of only 5 dBs is achieved when selected strongest MPCs are increased from 20 to 100.

correlation strength between the desired response $d_m(i)$ and the output $r_s(i)$ of ANC varying between +0.65 to +0.9 due to $\phi_m(i)$ is depicted in Fig. 5. It can be seen that even for $\phi_m(i)$ of less than 0.01, ANC still provides a correlation strength greater then 0.6 between the desired response and the output of ANC.

Although, in practical scenario the correlated noise samples for the reference signal can be obtained using a side lobe of an antenna array with the primary input being received from far field at the main lobe.

The adopted values of f_c and N_{cpb} for R_b the bit rate, T_c the chip duration and N_c the number of chips per symbol of channel 11 of [1] are mentioned in Table(I).
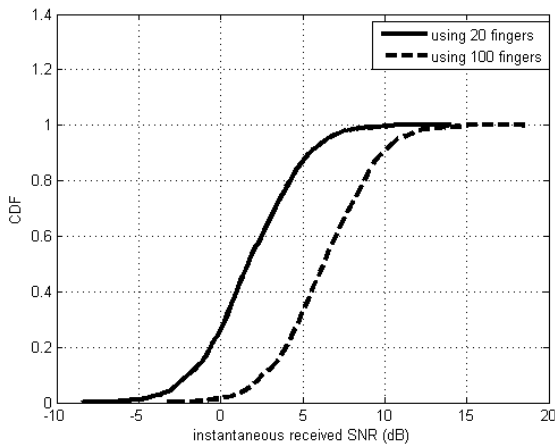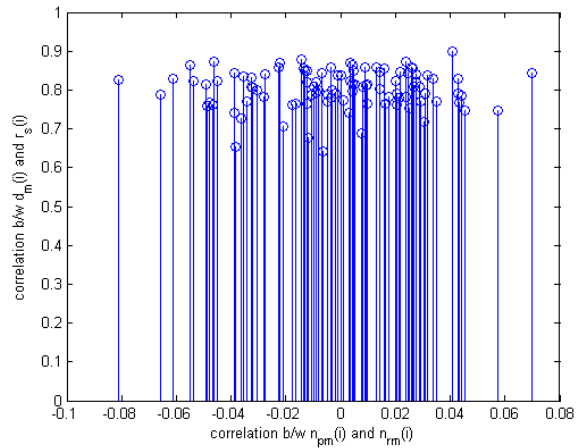

Fig. 4. The CDF of received instantaneous SNR obtained from 20 and 100 strongest MPCs of 1000 channel realizations of CM8. The average transmitted SNR=0 dB

TABLE I
PARAMETERS FOR CHANNEL 11

f_c(GHz)	R_b (Mb/s)	T_c (ns)	N_{cpb}	N_c	N_{hop}
7.987	0.85	2	16	256	8

Using the above parameters, the error performance of BPM-BPSK modulated IR-TH UWB biorthogonal signals was found in IEEE 802.15.4a industrial NLOS environment of CM8 in the presence of AWGN. Both the conventional SRake and robust SRake receivers employ 20 fingers in each Rake unit. An appreciable performance improvement is observed with a proposed robust SRake which provides a gain of approximately 33 dBs and 5 dBs respectively with the conventional SRake and AWGN correlation receivers as shown in Fig. 6. It is therefore suggested, that instead of using hundreds of Rake fingers, an addition of an ANC drastically improves the error performance of conventional SRake receiver in dense multipath propagated environment.

To simulate the performance of ANC, 1000 random samples of primary noise $n_{pm}(i)$ were generated and passed through a 32 order low pass filter (LPF) to obtain the respective correlated reference noise samples of $n_{rm}(i)$. A correlation strength $\varphi_m(i)$ ranging from -0.08 to +0.07 was obtained. For the simulation of RLS algorithm, Identity matrix $\mathbf{I}$ was selected as $\mathbf{\Phi_m}(y)$ of Eq.(19). The tap weight vector $\mathbf{w_m}(y)$ was initialized using all zeros vector with the exponential weighting factor $\alpha_m = 1$. To keep the recursions in progress and for the initial setting of the correlation matrix, $\mathbf{\Phi_m}(y)$ was multiplied with a small positive value $\delta_m = 0.1$.
Using $M_w = 32$ as the order of tap weight vector, the obtained

VI. CONCLUSION

The generated power delay profile of IEEE 802.15.4a industrial NLOS environment of CM8 exhibits dense multipath
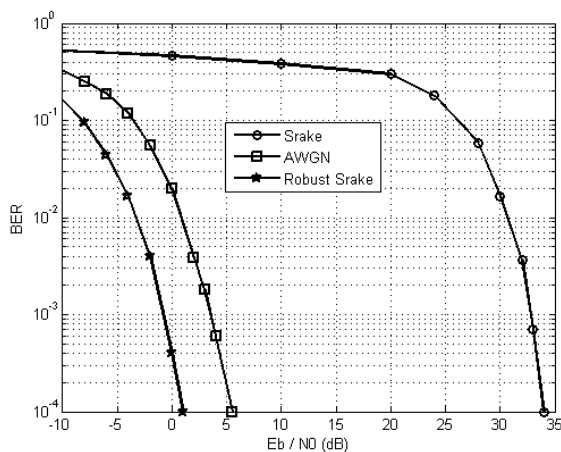
Fig. 6. BER vs SNR of uncoded IEEE 802.15.4a IR-TH UWB. SRake and robust SRake reception with 20 fingers: Average over 100 CM8 channel realizations in the presence of AWGN in comparison with correlation reception over AWGN

fading, with the first ray not carrying the highest magnitude. The number of resolvable multipath components increases with the bandwidth, for which plenty of diversity paths are needed to obtain an appreciable increase in instantaneous SNR. By including an adaptive noise canceler, the proposed robust SRake architecture with very less number of fingers, effectively recovered the weak BPM-BPSK modulated IR-TH UWB biorthogonal signals in CM8. The respective error performance depicts a significant improvement as compared to both the conventional SRake and AWGN receivers.

ACKNOWLEDGMENT

REFERENCES

[1] IEEE 802.15.4a-2007, "Part 15.4: Wireless Medium Access Control (MAC) and Physical Layer (PHY) Specifications for Low-Rate Wireless Personal Area Networks (WPANs); Amendment 1: Add Alternate PHYs," Mar. 2007.

[2] D. Dardari, C. C. Chong and M. Z. Win, "Threshold-Based Time-of-Arrival Estimators in UWB Dense Multipath Channels," *IEEE Transactions on Communications*, vol. 56, no. 8, pp. 1366–1378, August 2008.

[3] A. D. Reyna and I. A. Catalina, "Practical search strategy for ultra wideband signal acquisition in the dense multipath channel," *IEEE Mediterranean Electrotechnical Conference (MELECON)*, pp. 635–638, May 2006.

[4] M. Kim, H. Kim and J. Kim, "High-Level Modeling of UWB PHY for IEEE802.15.4a," *Convergence and Hybrid Information Technology (ICHIT)*, pp. 351–354, 2008.

[5] W. C. Liu and L. Wang, "BER Analysis of the IEEE 802.15.4a Channel Model with RAKE Receiver," *IEEE Vehicular Technology Conference (VTC Fall)*, pp. 1–5, 2006.

[6] W. c. Liu and L. C. Wang, "BER Analysis in a Generalized UWB Frequency Selective Fading Channel with Randomly Arriving Clusters and Rays," *IEEE International Conference on Communication (ICC)*, pp. 4281–4286, 2007.

[7] Z. Ahmadian and L. Lampe, "Performance Analysis of the IEEE 802.15.4a UWB System," *IEEE Transactions on Communications*, vol. 57, no. 5, pp. 1474–1485, 2009.

[8] H. Gong, H. Nie and Z. Chen, "Performance Comparisons of UWB Selective Rake and Transmitted Reference Receivers under IEEE802.15.4a Industrial Environments," *IEEE Wireless and Microwave Technology Conference (WAMICON)*, pp. 1–5, 2006.

[9] B. Widrow, J. R. Glover, J. M. McCool, J. Kaunitz, C. R. Williams, E. Dong and R. C. Goodlin, "Adaptive Noise Cancelling: Principles and Applications," *Proceedings of the IEEE*, vol. 63, no. 12, Dec. 1975.

[10] S. G. Glisic and P. A. Leppanen, *Wireless Communications: TDMA vs CDMA*, Kluwer Academic Publishers, 1997.

[11] A. F. Molisch, "Ultra-Wide-Band Propagation Channels" *Proceedings of the IEEE*, vol. 97, no. 2, pp. 353–371, 2009.

[12] J. Karedal, S. Wyne, P. Almers, F. Tufvesson and A. F. Molisch, "A measurement Based Statistical Model for Industrial Ultra Wideband Channels," *IEEE Transactions on Wireless Communication*, vol. 6, no. 8, 2007.

[13] A. F. Molisch, K. Balakrishnan, D. Cassioli, C. C. Chong, S. Emami, J. Karedal, A. Fort, B. Kanan, J. Kunisch, H. G. Schantz, K. Siwiak and M. Z. Win, "A Comprehensive Standardized Model for Ultrawideband Propagation Channels," *IEEE Transactions on Antenna and Propagation*, vol. , no. 11 Part 1, pp. 3151–3166, 2006.

[14] S. Haykin, *Adaptive Filter Theory; 3rd Edition*, Prentice Hall Information and System Sciences Series, 1996.

[15] A. F. Molisch, K. Balakrishnan, D. Cassioli, C. C. Chong, S. Emami and J. Karedal, "IEEE 802.15.4a Channel Model-final report," *Taskgroup 4a (TG4a), Tech. Report*, 2004.

Farah Haroon received her Masters of Electrical Engineering degree from NED University of Engineering and Technology, Pakistan in 2003. She is currently a PhD student in Telecommunications Field of Study, Asian Institute of Technology, Thailand. Her research interests are ultra wide band communication, propagation and reception in multipath fading channels and industrial wireless networks.

Haroon Rasheed is currently pursuing the Ph.D degree at Asian Institute of Technology Thailand. He received his B.E in Electronics engineering and M.Engg electrical engineering from NED university Pakistan in 1998 and 2003. He also received Master of engineering in telecommunications in 2009 from Asian Institute of Technology Thailand. His research interests span UWB, OFDM based wireless technologies including spectrum sensing and dynamic spectrum access in cognitive radio and cooperative networks.

Kazi Mohiuddin Ahmed received his M.Sc. Engg degree in Electrical Engineering from the Institute of Communications, Leningrad, USSR, and the PhD degree from the University of Newcastle, NSW, Australia, in 1978 and 1983, respectively. Currently, he is a Professor of telecommunications in School of Engineering and Technology, Asian Institute of Technology, Thailand. His current research interests include digital signal processing, antenna array processing, tropospheric and ionospheric propagation studies for Microwave, ultra wide band, very high frequency-ultrahigh frequency (VHF-UHF) communications, and satellite communications. Mr. Ahmed is a member of IEEE, IEICE and life member of Bangladesh Electronic Society (BES).